

RESOLUTION TEST CHART
1963-A

AD-A140 560

2

NAVY RESEARCH AND DEVELOPMENT CENTER



Washington, D.C. 20340

**WAVELENGTH FORMULATIONS FOR TURBULENT BOUNDARY
LAYERS OVER ARBITRARILY ROUGH SURFACES**

by

Paul S. Gnanou

APPROVED FOR PUBLIC RELEASE: DISTRIBUTION UNLIMITED

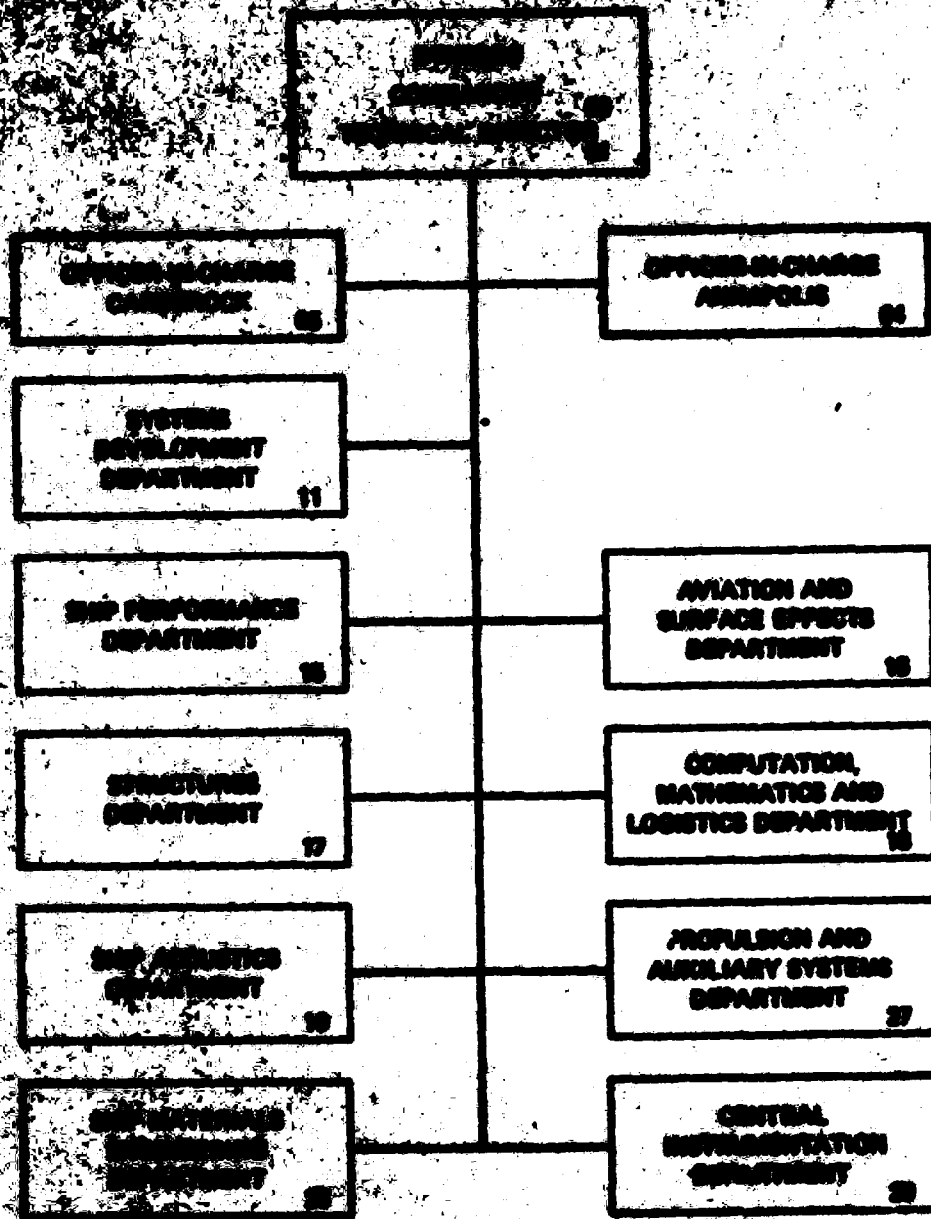
**DTIC
ELECTE
APR 27 1981**

**NAVY RESEARCH AND DEVELOPMENT CENTER
REPORT AND DEVELOPMENT REPORT**

NR 00000000

TURBULENT BOUNDARY LAYERS

GENERAL ORGANIZATIONAL COMPONENTS



UNCLASSIFIED

SECURITY CLASSIFICATION OF THIS PAGE (When Data Entered)

(Block 10)

Program Element 61135N
Task Area SR0230101
Work Unit 1542-070



Availability Codes	
Dist	Special
AI	

UNCLASSIFIED

SECURITY CLASSIFICATION OF THIS PAGE (When Data Entered)

TABLE OF CONTENTS

	Page
LIST OF FIGURES	iv
NOTATION	v
ABSTRACT	1
ADMINISTRATIVE INFORMATION	1
INTRODUCTION	1
CHARACTERIZATION OF ROUGHNESS DRAG	2
MIXING-LENGTH THEORY	4
EXISTING MIXING-LENGTH METHODS FOR ROUGH SURFACES	7
ROTTA I	7
ROTTA II	8
DAHM	9
PROPOSED NEAR-WALL MIXING LENGTHS FOR ROUGH SURFACES	10
GENERAL	10
INTERMEDIATE ROUGHNESS REGIME	10
FULLY ROUGH REGIME	11
GENERALIZED ROTTA II	11
DISCUSSION	11
NUMERICAL RESULTS	13
SUMMARY	14
APPENDIX A - CONVERSION OF MIXING LENGTHS TO EDDY VISCOSITIES	23
APPENDIX B - NEAR-WALL VALUES OF TURBULENT KINETIC ENERGY (k) AND TURBULENT DISSIPATION RATE (ϵ)	27
APPENDIX C - HYPERBOLIC-TANGENT MODIFICATION FUNCTION	31
REFERENCES	33

LIST OF FIGURES

	Page
1 - Variation of Integrand $y^* \left(\frac{dl_2^*}{dy^*} \right)$ with y^*	15
2 - Plot of λ_v^* versus B_1 for Intermediate Roughness Regime	16
3 - Plot of Rotta I l_w^* versus B_1 for Fully Rough Regime	17
4 - Correlation of Rotta II Factor Δy^* with B_1 for Intermediate Roughness Regime	18
5 - Correlation of Rotta II Factor Δy^* with B_1 for Fully Rough Regime	19
6 - Comparison of Rotta I and Rotta II Wall Mixing Lengths l_w^*	20
7 - Comparison of Mixing Lengths	21
A.1 - Eddy Viscosities Over Rough Surfaces	25
B.1 - Variation of Turbulent Kinetic Energy Near Wall	29
B.2 - Variation of Turbulent Dissipation Rate Near Wall	30
C.1 - Comparison of $y^* \left(\frac{dl_2^*}{dy^*} \right)$	32

NOTATION

A	Slope of logarithmic velocity law, $A = 1/\kappa$
B_1	Intercept of logarithmic velocity law in Reynolds-number mode (also drag characterization function)
$B_{1,s}$	Value of B_1 for smooth surfaces
B_r	Intercept of logarithmic velocity law in relative-roughness mode
\hat{B}_r	Value of B_r for fully rough regime
I_1, I_2	Integrals defined by Equation (30)
k	Roughness height
k_1, k_2, \dots	Other roughness lengths
k^*	Roughness Reynolds number, $k^* = u_\tau k/\nu$
k	Turbulent kinetic energy
l	Mixing length
l^*	Nondimensional mixing length, $l^* = u_\tau l/\nu$
l_v^*	Value of l^* at the wall
M	Modification function
T	Roughness texture, $T = k/k_1, k_1/k_2, \dots$
u	Streamwise velocity component
u^*	Nondimensional u, $u^* = u/u_\tau$
u_τ	Shear velocity, $u_\tau = \sqrt{\tau_w/\rho}$
w	Subscript denoting conditions at the wall, $y = 0$
y	Normal distance from wall

y^*	Nondimensional y , $y^* = u_T y / \nu$
y_L	Laminar sublayer thickness
y_L^*	Nondimensional y_L , $y_L^* = u_T y_L / \nu$
ΔB	Drag characterization, $\Delta B = B_1 - B_{1,s}$
Δy^*	Rotta II shift
ϵ	Turbulent dissipation rate
κ	von Kármán constant
λ	Length factor in modification function
λ^*	Nondimensional λ , $\lambda^* = u_T \lambda / \nu$
λ_h^*	λ^* for hyperbolic-tangent modification function
λ_v^*	λ^* for van Driest modification function
$\lambda_{v,s}^*$	λ_v^* for smooth surfaces
ν	Kinematic viscosity of fluid
ν_t	Turbulent eddy viscosity
ρ	Density of fluid
τ	Shearing stress
τ_l	Laminar shearing stress
τ_t	Turbulent shear stress
τ_w	Wall shearing stress

ABSTRACT

Mixing lengths are formulated for turbulent boundary layers over arbitrarily rough surfaces from both the van Driest and from the Rotta procedures. The associated eddy viscosities and the associated turbulent kinetic energies and turbulent dissipation rates are also formulated.

ADMINISTRATIVE INFORMATION

The work in this report was performed at the David W. Taylor Naval Ship Research and Development Center. It was authorized and funded by the General Hydromechanics Program of the Naval Sea Systems Command under Program Element 61135N, Task Area SR0230101, and Work Unit 1542-070.

INTRODUCTION

The development of turbulent boundary layers over arbitrarily rough surfaces may be predicted by mixing-length formulations close to the boundary wall. Existing calculation methods for smooth surfaces using the Prandtl-van Driest wall mixing length may be adapted to arbitrarily rough surfaces. Such methods for smooth surfaces are the method of Patankar and Spalding,¹ the method of Cebeci and Smith,² or its subsequent modification by Nituch et al.³ and the method of Huang et al.⁴

Wall mixing lengths, or rather the associated eddy viscosities, are also required for heat or mass transfer methods using turbulent Prandtl numbers or turbulent Schmidt numbers to predict the turbulent diffusivities of heat or mass.⁵ Furthermore, mixing lengths or eddy viscosities near the wall may be required as boundary conditions to the k - ϵ transport equations for improved predictions of the development of turbulent boundary layers.⁶ In general, the mixing length increases with distance away from the wall until a limiting value is reached which is compatible to the mixing length for the outer region.

Initially, in 1950, Rotta⁷ considered the Prandtl wall mixing length for turbulent shear stress to apply only outside the laminar sublayer and was able to correlate the laminar sublayer thickness with the roughness drag characterization function. However, subsequent turbulence measurements showed that turbulent shear stresses start at the wall. The concept of a purely laminar sublayer was discarded and the laminar sublayer was renamed the viscous sublayer. For smooth surfaces, the

*A complete listing of references is given on page 33.

van Driest modification to the Prandtl wall mixing-length formulation provided a turbulent shear stress which started at the wall. Rotta⁸ then adapted the van Driest-Prandtl mixing length for smooth surfaces to rough surfaces by shifting the position of the reference wall an appropriate distance. Rotta presented the numerical results in graphical form for two well-known roughnesses: the Nikuradse sand-grain roughness and the Colebrook-White engineering roughness. Later Cebeci and Smith² provided an analytical fit to the wall shift for the sand-grain roughness which was then used by Cebeci and Chang⁹ for calculations of turbulent boundary layers over rough surfaces.

For arbitrarily rough surfaces, the van Driest factor is correlated in this paper with the roughness drag characterization function until a limiting value of zero is reached. This is considered to represent the beginning of the fully rough regime. Then, for the fully rough regime, the mixing length is considered to assume an initial value at the wall in accordance with Rotta's original (1950) analysis.

For purposes of comparison, the second Rotta analysis of a wall shift is generalized to produce numerical results for the drag characterization of arbitrary roughness. In Appendix A, an explicit conversion of mixing-lengths to eddy viscosities is derived. In Appendix B, the associated turbulent kinetic energies (ϵ) and turbulent dissipation rate (ϵ) are developed.

CHARACTERIZATION OF ROUGHNESS DRAG

A brief review is presented of pertinent features of the velocity similarity laws and the associated drag characterizations of rough surfaces.

Close to the wall, the logarithmic velocity law for an arbitrarily rough surface, defined by a sufficient number of length factors k, k_1, k_2, \dots , is given in what may be called the Reynolds-number mode as

$$\frac{u}{u_\tau} = A \ln y^+ + B_1 [k^+, T] \quad (1)$$

and, in what may be called the relative-roughness mode, as

$$\frac{u}{u_\tau} = A \ln \frac{y}{k} + B_r [k^+, T] \quad (2)$$

where

$$B_T = B_1 + A \ln k^* \quad (3)$$

Here u = streamwise velocity component

u_T = shear velocity, $u_T = \sqrt{\tau_w/\rho}$

τ_w = wall shear stress

ρ = density of fluid

y^+ = $u_T y/\nu$

y = normal distance from wall

ν = kinematic viscosity of fluid

T = texture of roughness configuration, $T = k/k_1, k_1/k_2, \dots$

k^* = roughness Reynolds number, $k^* = u_T k/\nu$

Either B_1 or B_T may be considered to be a roughness drag characterization function. Both B_1 and B_T are functions of roughness Reynolds number k^* and texture T .

The usual roughness regimes are

1. Hydraulically smooth

$$B_1 = B_{1,s} = \text{constant} \quad (4)$$

$$B_T = B_{1,s} + A \ln k^*$$

2. Intermediate roughness

Both B_1 and B_T vary with k^* for the same T

3. Fully rough

$$B_T = B_T(T) = \text{constant}$$

$$B_1 = B_T(T) - A \ln k^* \quad (5)$$

Another drag characterization is given by ΔB which represents a deviation from smooth conditions or

$$\Delta B [k^*, T] = B_{1,r} [k^*, T] - B_{1,s} \quad (6)$$

As defined, ΔB is always negative for rough surfaces. Nikuradse¹⁰ used the $B_{1,r}$ -characterization while Hama¹¹ preferred the ΔB (actually $-\Delta B$) characterization.

To experimentally determine a characterization for a specific arbitrarily rough surface, there are various procedures available. The direct procedure requires velocity measurements close to the wall to define a logarithmic law as well as the measurement of the wall shear stress. Simpler, indirect procedures may be used involving measurement of the average velocity of pipe flow,¹⁰ the total drag of a flat plate,¹² or the torque of a rotating disk.¹³

MIXING-LENGTH THEORY

According to the Prandtl mixing-length theory, the turbulent shear stress (τ_t) is related to the velocity gradient by

$$\frac{\tau_t}{\rho} = l^2 \left(\frac{du}{dy} \right)^2 \quad (7)$$

where l is the mixing length which, in general, is not constant, but is a function of its position in the flow field.

The total shear stress τ at a point in the flow field is the sum of laminar τ_l and turbulent τ_t shear stresses or

$$\tau = \mu \frac{du}{dy} + l^2 \left(\frac{du}{dy} \right)^2 \quad (8)$$

where $\frac{\tau_l}{\mu} = \frac{du}{dy}$, the Newtonian Law of Viscosity.

For a shear layer with zero longitudinal pressure gradient, $\tau = \tau_w$ close to the wall. With this approximation, Equation (8) may be written in a nondimensional form

$$l^{*2} \left(\frac{du^*}{dy^*} \right)^2 + \frac{du^*}{dy^*} = 1 \quad (9)$$

where l^* is a nondimensional mixing length, $l^* = u_T l / \nu$, and u^* is a nondimensional velocity, $u^* = u / u_T$.

Solving for du^*/dy^* as a quadratic expression and integrating from the wall, where $y^* = 0$ and $u^* = 0$, results in a velocity profile

$$u^* = \int_0^{y^*} \frac{2}{1 + \sqrt{1 + (2l^*)^2}} dy^* \quad (10)$$

Close to the wall Prandtl proposed a linear variation of mixing length with distance from the wall

$$l^* = \kappa y^* \quad (11)$$

where κ is the von Kármán constant. Use of this relation, in Equation (10), leads to a logarithmic velocity law with $A = 1/\kappa$. However, an erroneous value of B_1 results. Furthermore, in so far as the logarithmic velocity law does not hold right up to the wall, so the Prandtl wall mixing length does not hold. To remedy this, a modification function $M(i^* = \kappa y^*)$ is needed as a function of y^* and i^* where i^* is an additional nondimensional length, $i^* = u_T i / \nu$. Furthermore, M should equal zero at $y^* = 0$ and equal unity at $y^* \rightarrow \infty$.

For smooth surfaces, van Driest proposed¹⁴ the representation

$$M = 1 - \exp\left(\frac{-y^*}{\lambda_v^*}\right) \quad (12)$$

where λ_v^* is the λ^* associated with van Driest.

Other modification functions may be formulated as, for example, the hyperbolic tangent function alluded to by Patel¹⁵

$$M = \sqrt{\tanh\left(\frac{y^*}{\lambda_h^*}\right)^2} \quad (13)$$

where λ_h^* is the λ^* used here.

Why M should equal zero at $y^* = 0$ requires some further discussion. Theoretical investigations⁵ indicate that the eddy viscosity ν_t should vary with y^{*3} or y^{*4} at $y^* = 0$. Now Equation (A.6) in Appendix A relates the eddy viscosity to the mixing length. A Maclaurin expansion gives

$$\frac{\nu_t}{\nu} = 2 \lambda^{*2} + \dots \quad (14)$$

or

$$\frac{\nu_t}{\nu} = 2\kappa^2 y^{*2} M^2 + \dots$$

A nonzero value of M at $y^* = 0$ such as M_1 would then result in

$$\frac{\nu_t}{\nu} = 2\kappa^2 M_1^2 y^{*2} + \dots \quad (15)$$

which is not acceptable.

A Maclaurin expansion of the van Driest M gives

$$M = \frac{y^*}{\lambda_v^*} + \dots \quad (16)$$

and

$$\frac{\nu_t}{\nu} = \frac{2\kappa^2}{\lambda_v^{*2}} y^{*4} + \dots \quad (17)$$

which is acceptable.

Likewise, for the hyperbolic tangent M

$$\frac{v}{v} = \frac{2\kappa^2}{\lambda h} y^{*4} + \dots \quad (18)$$

EXISTING MIXING-LENGTH METHODS FOR ROUGH SURFACES

Some pertinent existing mixing-length methods for rough surfaces are now critically examined.

ROTTA 1

An extension of the Prandtl wall mixing length method to rough surfaces, initially proposed by Rotta,⁷ assumed a laminar sublayer thickness that would decrease with roughness or

$$l^* = \kappa(y^* - y_L^*) \quad (19)$$

where y_L is the laminar sublayer thickness and $y_L^* = u_\tau y_L / \nu$. The introduction of l^* in Equation (10) resulted in an integration in elementary functions and a relation between y_L^* and B_1

$$y_L^* = B_1 + \frac{1}{\kappa} (1 - \ln 4\kappa) \quad (20)$$

With increasing roughness, the laminar sublayer finally vanishes, $y_L^* = 0$, and $B_1 = -1/\kappa (1 - \ln 4\kappa)$. This is now considered to be the beginning of the fully rough regime and the end of the intermediate roughness regime.

For the fully rough regime, Rotta assumed an initial mixing length l_w^* at the wall

$$l^* = l_w^* + \kappa y^* \quad (21)$$

The introduction of this mixing length for the fully rough regime into the velocity profile, Equation (10), results in an analytical solution.

$$\begin{aligned}
u^* &= \frac{1}{\kappa l^*} \left(\frac{1}{2} - \sqrt{l^{*2} + \frac{1}{4}} \right) - \frac{1}{\kappa l_w^*} \left(\frac{1}{2} - \sqrt{l_w^{*2} + \frac{1}{4}} \right) \\
&+ \frac{1}{\kappa} \ln \left(\frac{l^* + \sqrt{l^{*2} + \frac{1}{4}}}{l_w^* + \sqrt{l_w^{*2} + \frac{1}{4}}} \right)
\end{aligned} \tag{22}$$

At higher values of y^* , this relation reduces to the usual log law, Equation (1), so that

$$\begin{aligned}
B_1 &= \frac{1}{\kappa} (\ln 4\kappa - 1) - \frac{1}{\kappa l_w^*} \left(\frac{1}{2} - \sqrt{l_w^{*2} + \frac{1}{4}} \right) \\
&- \frac{1}{\kappa} \ln \left(2l_w^* + 2\sqrt{l_w^{*2} + \frac{1}{4}} \right)
\end{aligned} \tag{23}$$

This relates B_1 and l_w^* ; therefore, the velocity profile, Equation (10), is a function of y^* and B_1 .

ROTTA II

Rotta⁸ seems to have abandoned the laminar sublayer approach in analyzing rough surfaces after the whole concept of a purely laminar flow next to the wall became untenable. Since there are turbulent stresses even in the laminar sublayer, the sublayer has been renamed the viscous sublayer.

Rotta extended the van Driest formulation for smooth surfaces to rough surfaces by adding a length Δy to the y coordinate such that

$$l^* = \kappa (y^* + \Delta y^*) \left\{ 1 - \exp \left[\frac{-(y^* + \Delta y^*)}{\lambda_{v,s}^*} \right] \right\} \tag{24}$$

where $\lambda_{v,s}^*$ is the value of λ_v^* for smooth surfaces. When this mixing length is incorporated into the velocity profile, Equation (10), and related to the logarithmic law, Equation (1), Δy^* becomes a function of $B_1[k^*, T]$. Instead of solving the general case of $\Delta y^* = f[B_1]$, Rotta solved $\Delta y^* = f[k^*]$ for the Nikuradse sand-grain roughness and $\Delta y^* = f[k^*]$ for the Colebrook-White engineering roughness and presented the results graphically. Cebeci and Smith² fitted the results for the Nikuradse sand-grain roughness to an empirical formula. Subsequently, Cebeci and Chang⁹ used this formula in boundary-layer calculations.

The Rotta formulation leads to an initial value of l^* , namely, l_w^* at the wall (for $y^* = 0$) or

$$l_w^* = \kappa \Delta y^* \left[1 - \exp\left(\frac{-\Delta y^*}{\lambda_{v,s}^*}\right) \right] \quad (25)$$

Hence $l_w^* = f[B_1] = f[k^*, T]$ for all roughness regimes.

DAHM

Dahm¹⁶ proposed a differential equation for the mixing lengths of rough surfaces based on empirical considerations, which, for zero mass injection, becomes

$$\frac{dl^*}{dy^*} = \frac{0.4 y^* - (l^* - l_w^*)}{11.83} \quad (26)$$

Examination indicates that this equation is a linear differential equation with a solution given by

$$l^* = 0.4 y^* + l_w^* + (0.4) (11.83) \left(\frac{1}{e^{y^*/11.83}} - 1 \right) \quad (27)$$

It may be noted that this formula resembles that of Rotta, Equation (21), for the fully rough regime ($\kappa=0.4$; also at $y^*=0$, and $l^*=l_v^*$). In actual use, values of l_v^* would have to be correlated with drag characterization (B_1).

PROPOSED NEAR-WALL MIXING LENGTHS FOR ROUGH SURFACES

GENERAL

Equating the velocity profiles obtained from mixing lengths, Equation (10), and the logarithmic law, Equation (1), produces

$$B_1 = \int_0^{\tilde{y}^*} \frac{2}{1 + \sqrt{1+(2l^*)^2}} dy^* - \frac{1}{\kappa} \ln \tilde{y}^* \quad (28)$$

and with

$$\ln \tilde{y}^* = \int_1^{\tilde{y}^*} \frac{dy^*}{y^*} \quad (29)$$

$$B_1 = \int_0^1 \frac{2}{1 + \sqrt{1+(2l^*)^2}} dy^* + \int_1^{\tilde{y}^*} \left[\frac{2}{1 + \sqrt{1+(2l^*)^2}} - \frac{1}{\kappa y^*} \right] dy^* \quad (30)$$

or

$$B_1 = I_1 + I_2 \quad (31)$$

where \tilde{y}^* is a sufficiently large value of y^* so that the second integrand of Equation (30), dI_2/dy^* , becomes negligible.

INTERMEDIATE ROUGHNESS REGIME

With the Prandtl-van Driest mixing length,

$$l^* = \kappa y^* \left[1 - \exp\left(\frac{-y^*}{\lambda_v^*}\right) \right] \quad (32)$$

in Equation (30), the van Driest factor λ_v^* becomes a function of B_1 and, hence, a function of roughness factors, k^* and T or $\lambda_v^* = f[B_1] = f[k^*, T]$.

Numerically then, λ_v^* from the preceding equation decreases with decreasing values of B_1 until the limit $\lambda_v^* = 0$ is reached. Then, $l^* = \kappa y^*$. This is the same limit as Rotta I where the laminar sublayer disappears.

The range of λ_v^* from its smooth value of $\lambda_{v,s}^*$ to its zero limit, may be considered to cover the intermediate roughness regime, at $\lambda_{v,s}^* > \lambda_v^* > 0$.

FULLY ROUGH REGIME

The original Rotta I proposal of an initial mixing length l_w^* at the wall for the fully rough regime will now be considered appropriate. Accordingly, Equations (11), (22), and (23) apply.

GENERALIZED ROTTA II

In order to make comparisons, the Rotta II method of an additional length Δy is now generalized. The Rotta II mixing length for rough surfaces, Equation (24), is substituted into either Equation (28) or (30) for B_1 so that Δy^* becomes a function of B_1 , so that $\Delta y^* = f[B_1] = f[k^*, T]$.

DISCUSSION

Two methods have been described for the prediction of mixing lengths for arbitrarily rough surfaces. There is the Rotta II method which is generalized in terms of the roughness characterization function and applies to both the intermediate and fully rough regimes. The Rotta II method extends the van Driest formula for smooth surfaces to rough surfaces by means of a normal distance parameter.

The other method described consists of an extension of the van Driest formula to the intermediate roughness regime; the van Driest factor is correlated to the roughness characterization function. For the fully rough regime the Rotta I method is to be used in which a wall mixing length is related to the roughness characterization function. The relative merits of each method are now discussed.

For the intermediate roughness regime, the Rotta II method leads to an initial mixing length, Equation (25), at the wall while the van Driest factor method gives

a zero mixing length. A nonzero mixing length at the wall implies the existence of a nonzero turbulent shear stress and a nonzero eddy viscosity at the wall as is demonstrated next.

Now the turbulent shear stress near the wall, Equation (7), nondimensionalized to

$$\frac{\tau_t}{\tau_w} = l^{*2} \left(\frac{du^*}{dy^*} \right)^2 \quad (33)$$

becomes, by use of Equation (10) for du^*/dy^*

$$\frac{\tau_t}{\tau_w} = \left[\frac{2l^*}{1 + \sqrt{1 + (2l^*)^2}} \right]^2 \quad (34)$$

then, at the wall $y^* = 0$,

$$\left(\frac{\tau_t}{\tau_w} \right)_w = \left[\frac{2l_w^*}{1 + \sqrt{1 + (2l_w^*)^2}} \right]^2 \quad (35)$$

Consequently, at the wall, the Rotta II method has a wall value of turbulent shear stress, but the van Driest factor method has none.

Also for the eddy viscosity, Equation (A.6) gives

$$\left(\frac{\nu_t}{\nu} \right)_w = \frac{1}{2} \sqrt{1 + (2l_w^*)^2} - \frac{1}{2} \quad (36)$$

Again, the Rotta II method has an initial value of eddy viscosity at the wall while the van Driest factor method has none. In fact, the van Driest factor method applied to the intermediate rough regime retains the variation of eddy viscosity with y^{*4} at the wall.

For the intermediate roughness regime, an initial value of mixing length, turbulent shear stress, and eddy viscosity at the wall may all be considered objectionable.

NUMERICAL RESULTS

In determining B_1 from an integration of mixing lengths by means of Equation (30), it is necessary to specify a limiting value of \bar{y}^* so that the integrand of I_2 becomes practically zero. As an example, the integrand $y^* (dI_2/dy^*)$ is plotted in Figure 1 for the smooth case $\lambda_v^* = 26$ and for the case of the beginning of the fully rough regime $\lambda_v^* = 0$ with $\kappa = 0.4$ (the same case as for ROTTA II). To compensate for the logarithmic abscissa, the ordinate is multiplied by y^* so that the area under the curve represents the integral I_2 . Then, $dI_2/dy^* = y^* (dI_2/dy^*) (d \ln y^*/dy^*)$. At values of y^* above about 200 the integrand is close to zero.

In Figure 2, the van Driest factor λ_v^* is correlated with drag characterization function B_1 for the intermediate roughness regime by means of Equation (35). This accommodates any arbitrary roughness. The limiting value is $B_1 = -1.325$ for $\lambda_v^* = 0$. Smaller values of B_1 are then in the fully rough regime.

The wall mixing length l_w^* for the fully rough regime is plotted against the drag characterization function B_1 in Figure 3 in accordance with the Rotta I relation, Equation (23).

In Figures 4 and 5 the Rotta factor Δy^* is plotted against the drag characterization function B_1 , as a result of solving Equations (24) and (30). This correlation applies to any arbitrary rough surface and, consequently, includes the Nikuradse sand-grain roughness and the Colebrook-White roughness.

A comparison is shown in Figure 6 for the mixing length l_w^* at the wall as a function of the roughness characterization function B_1 . It should be noted that the Rotta II formulation has values of l_w^* in the intermediate roughness regime in accordance with Equation (25). On the other hand, the van Driest formulation has a zero value. For the fully rough regime the Rotta I values are compared to the Rotta II values of l_w^* .

A comparison of the variation of mixing lengths l^* with normal distance y^* is displayed in Figure 7 for various formulations on the basis of equal values of B_1 . The smooth case is shown for a van Driest factor of 26. As an example of the intermediate roughness regime, a comparison is shown between the van Driest and

Rotta II formulations for $B_1 = 2$. It is to be noted that the Rotta II value of the mixing length is larger close to the wall. This is a result of having an initial value l_w^* at the wall. Mixing lengths at the border between the intermediate roughness and fully rough regimes are also compared. Here $\lambda_v^* = 0$ and $B_1 = -1.325$. For the fully rough regime, an example comparison is shown for $B_1 = -6$. It is to be further noted that for large values of y^* all the values of l^* tend to converge to the original Prandtl wall mixing length of $l^* = \kappa y^*$ as expected.

SUMMARY

For arbitrarily rough surfaces, two procedures have been developed. First is the extension of the Prandtl-van Driest formulation, Equation (12), to the intermediate roughness regime. Here the van Driest factor λ_v^* is correlated with drag characterization B_1 in Figure 2. For the fully rough regime, the Rotta I procedure may be used as given by Equation (23) which is plotted in Figure 3 as l_w^* against B_1 . Second, there is the Rotta II correlation, Equation (24), developed for arbitrarily rough surfaces. Figure 4 shows the correlation of Δy^* with B_1 for the intermediate roughness regime and Figure 5 shows that for the fully rough regime.

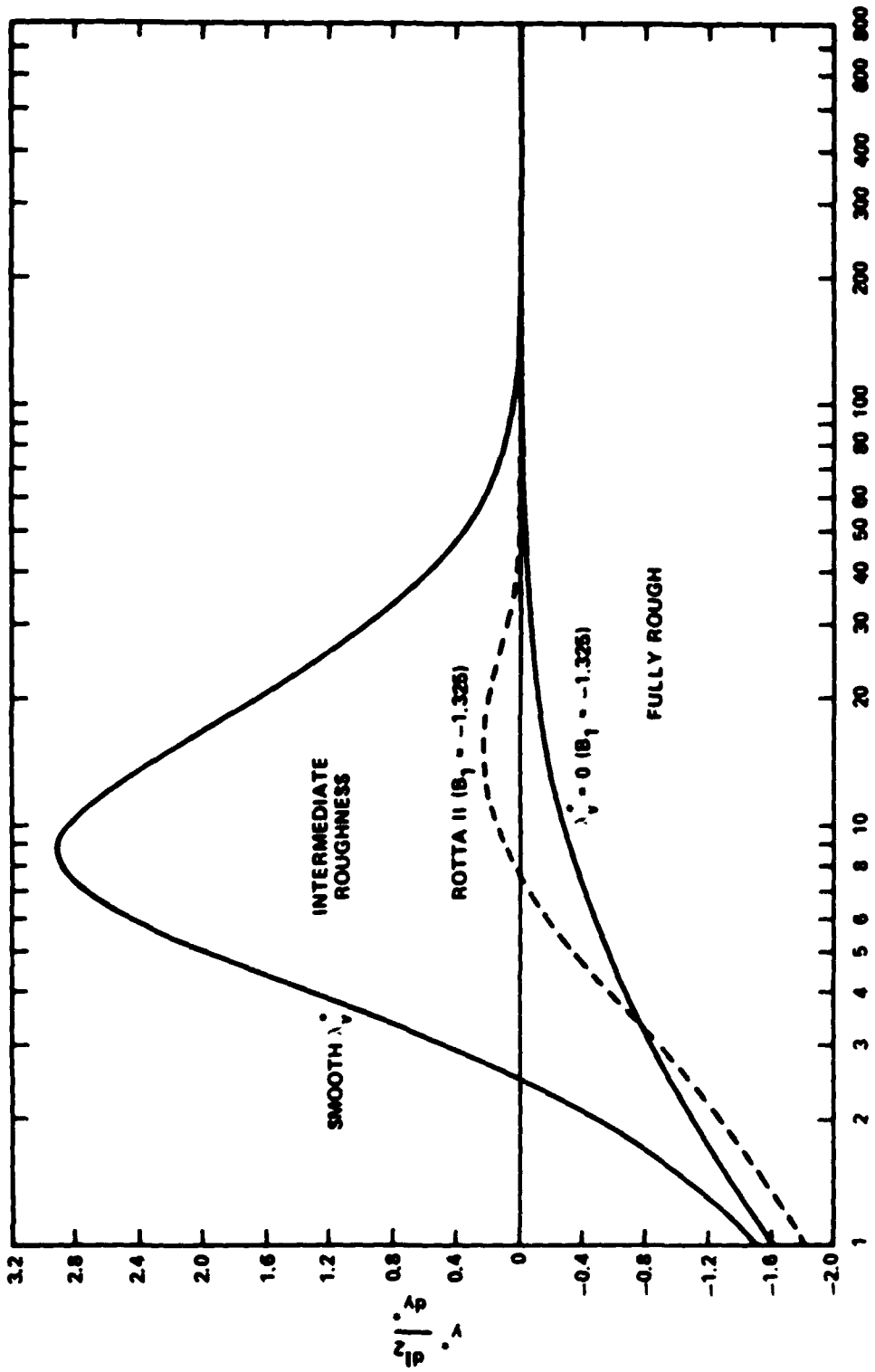


Figure 1 - Variation of Integrand $y'' \left(\frac{dy}{dx} \right)''$ with y''

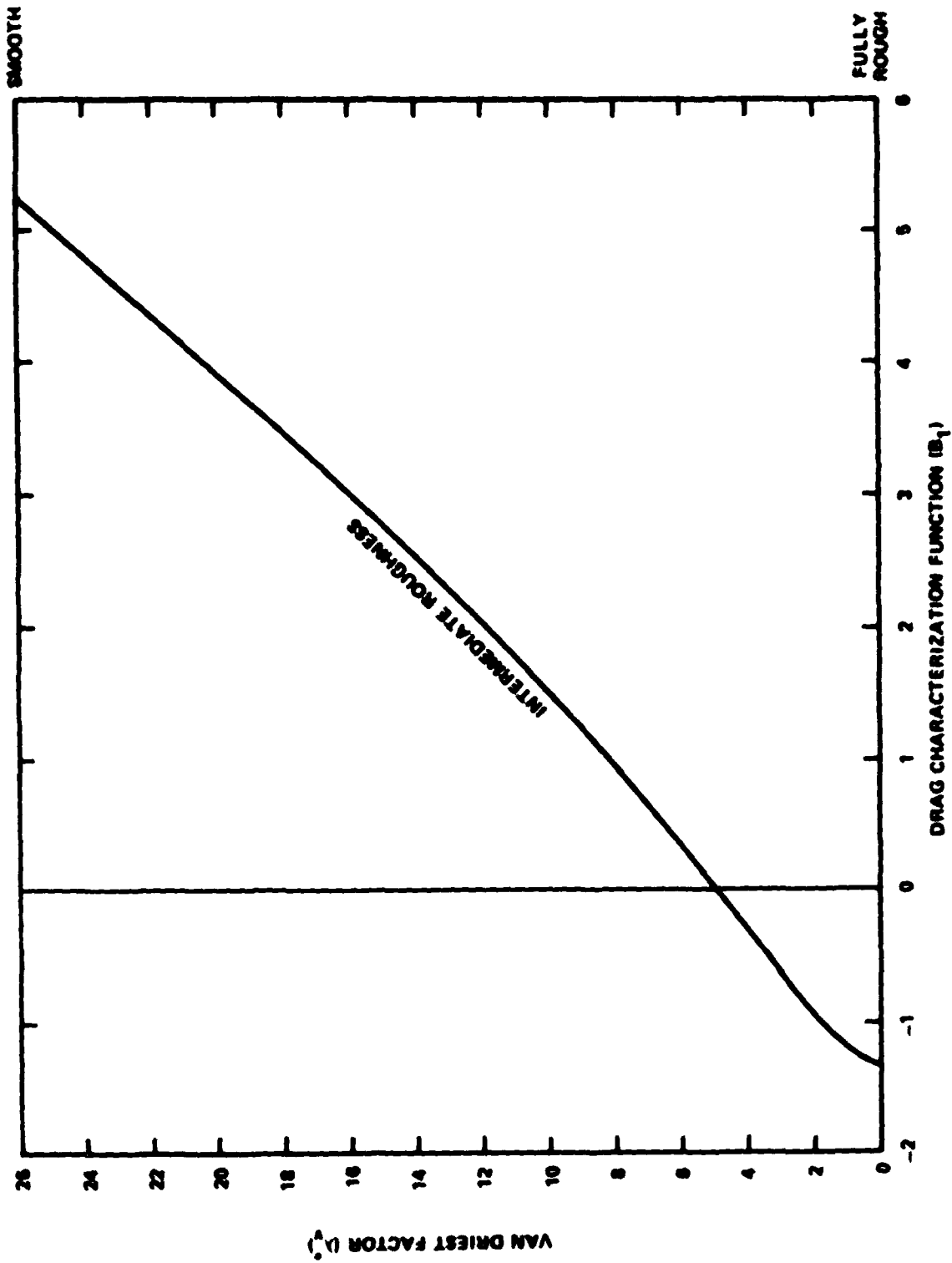


Figure 2 - Plot of U^+ versus B_1 for Intermediate Roughness Regime

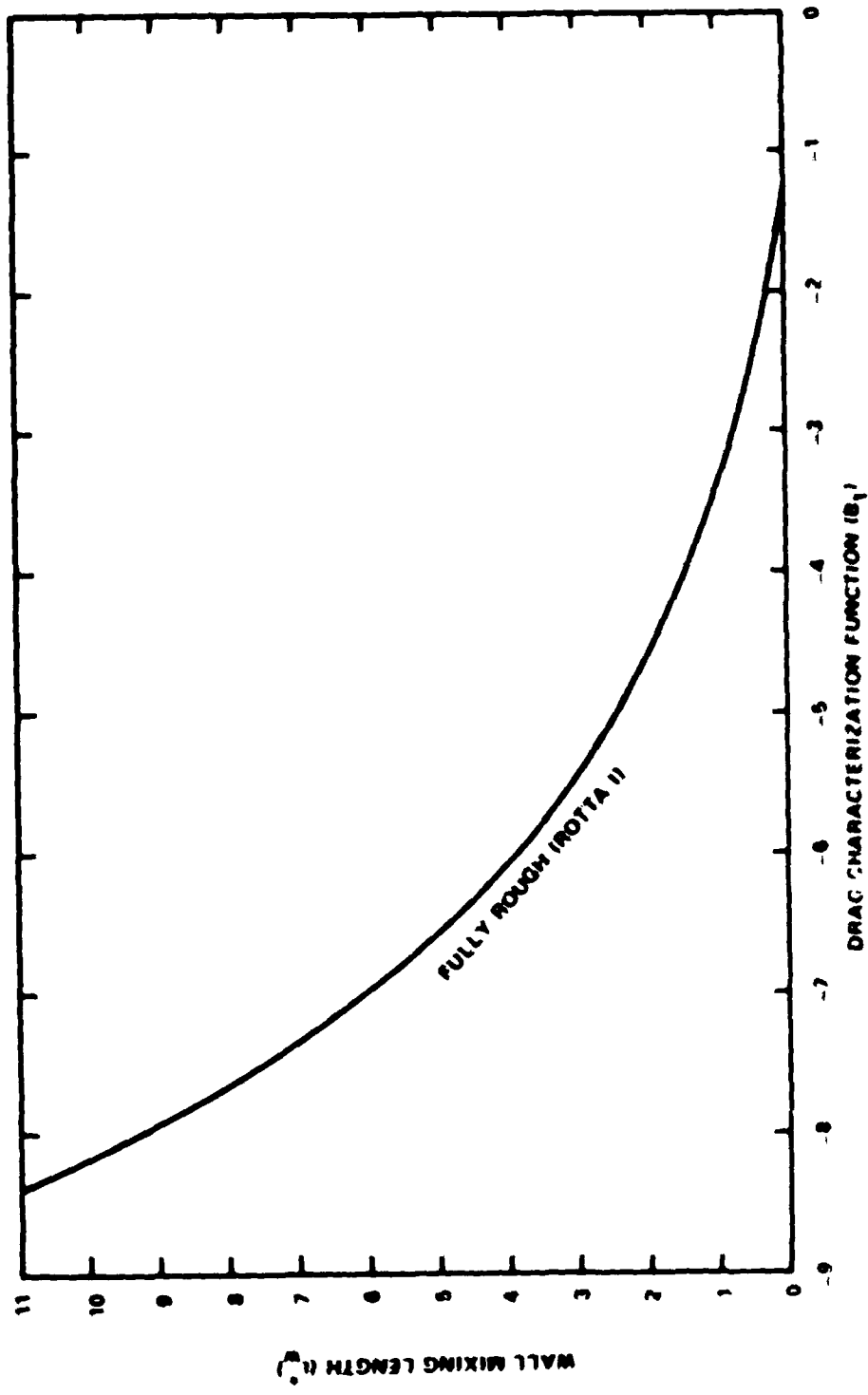


Figure 1 - Plot of Rotta L_w^+ versus B_1 for Fully Rough Regime

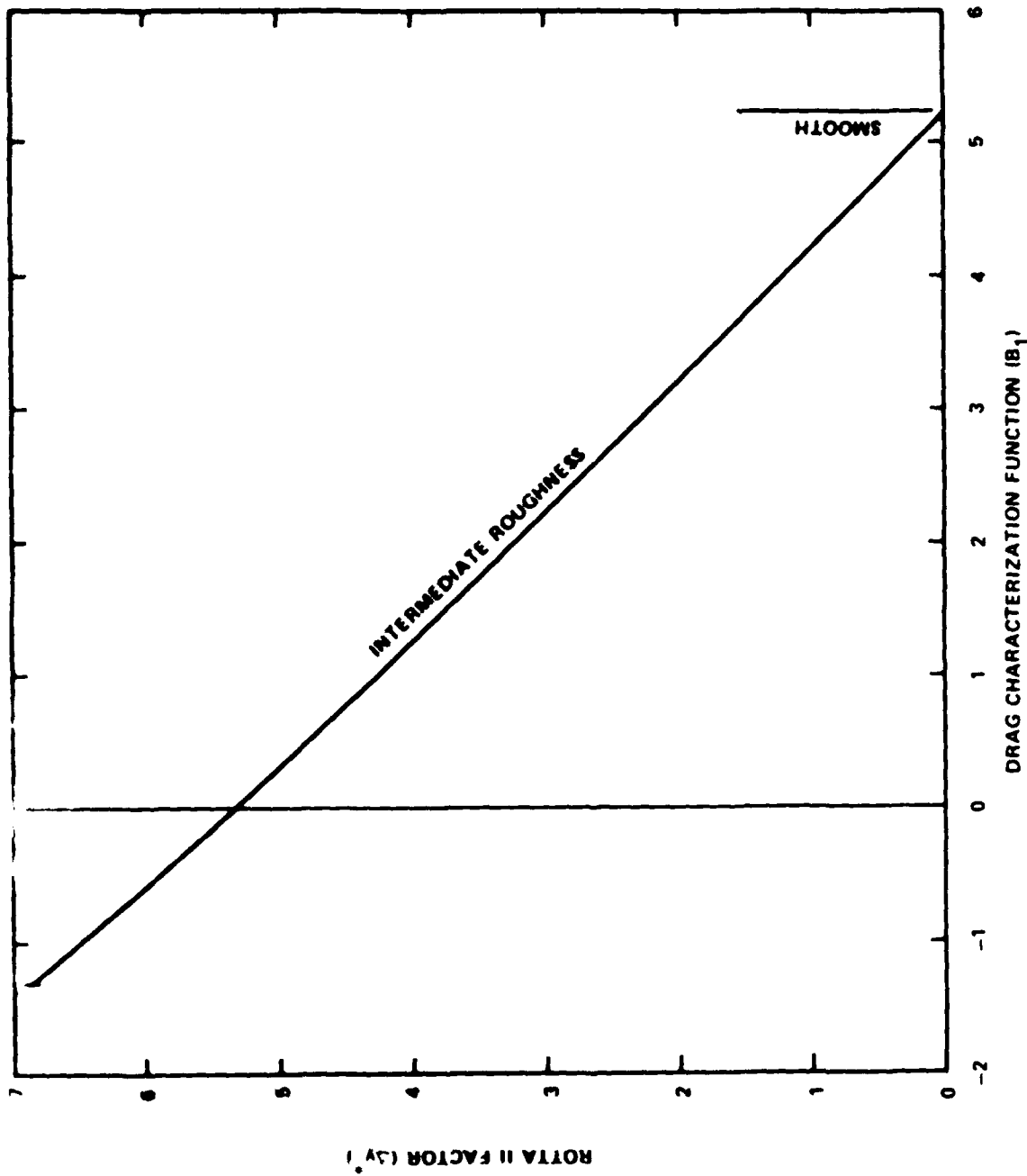
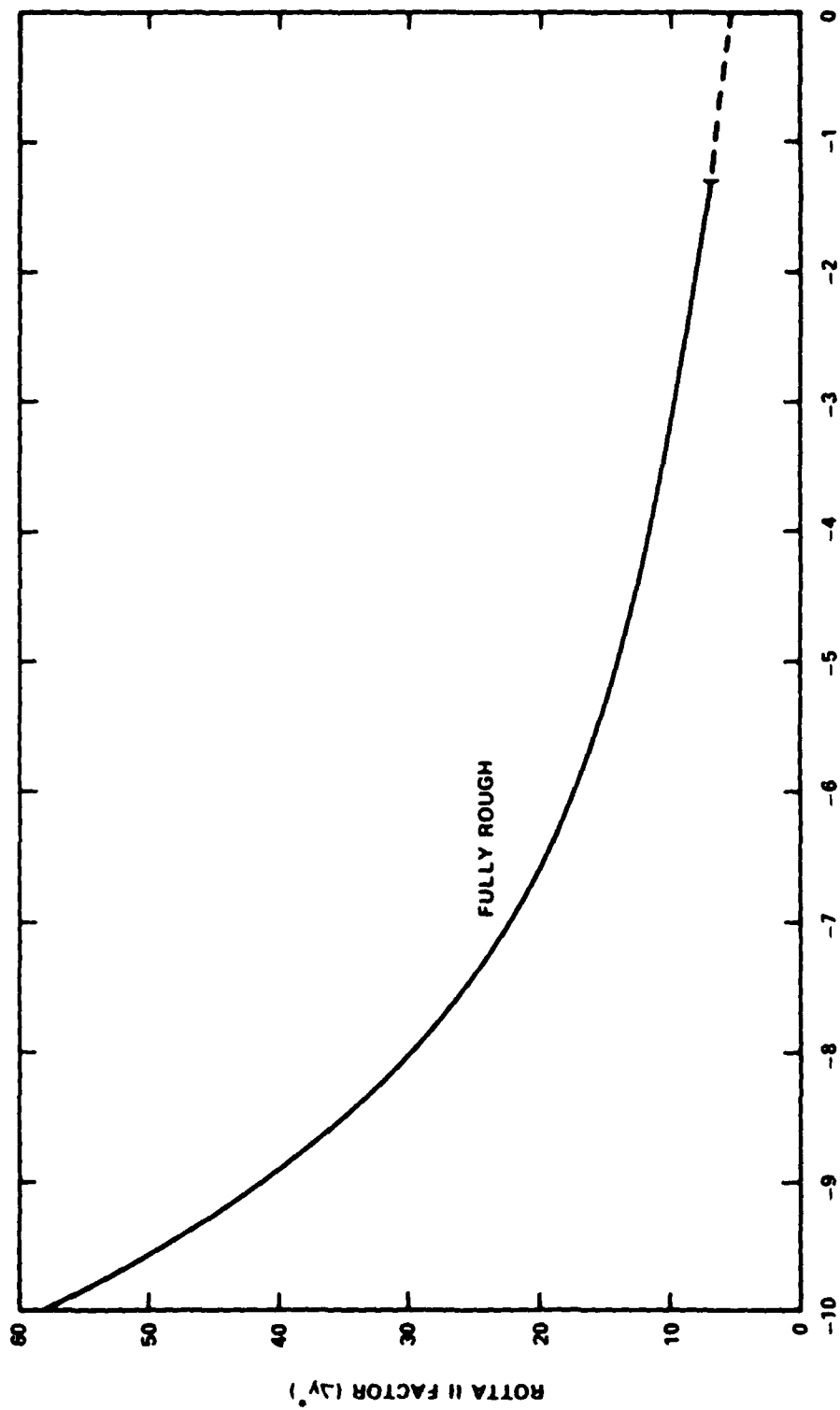


Figure 4 - Correlation of Rotta II Factor Δy^+ with B_1 for Intermediate Roughness Regime



DRAG CHARACTERIZATION FUNCTION (B_1)

Figure 5 - Correlation of Rotta II Factor ΔV^* with B_1 for Fully Rough Regime

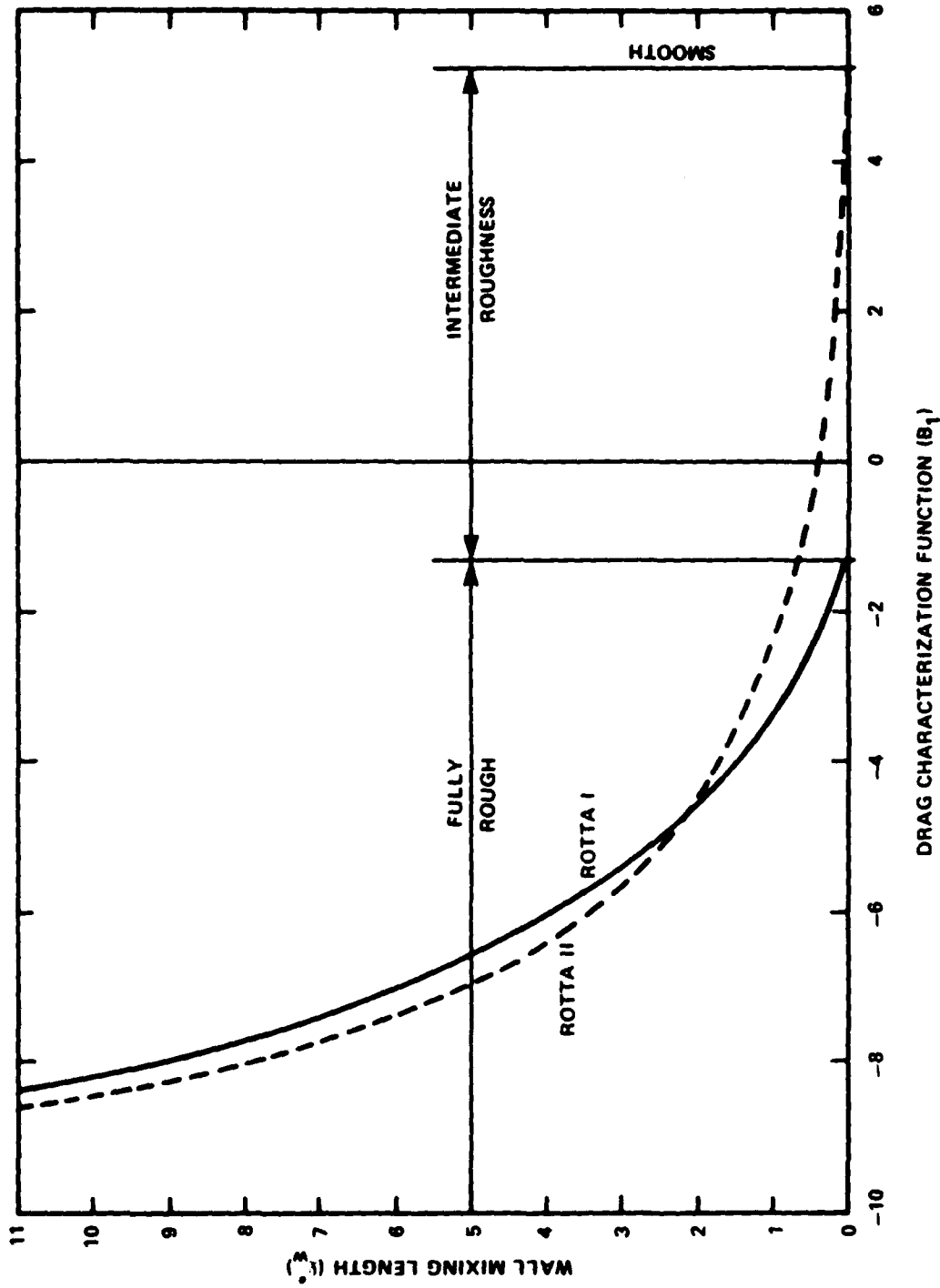


Figure 6 - Comparison of Rotta I and Rotta II Wall Mixing Lengths L_w^*

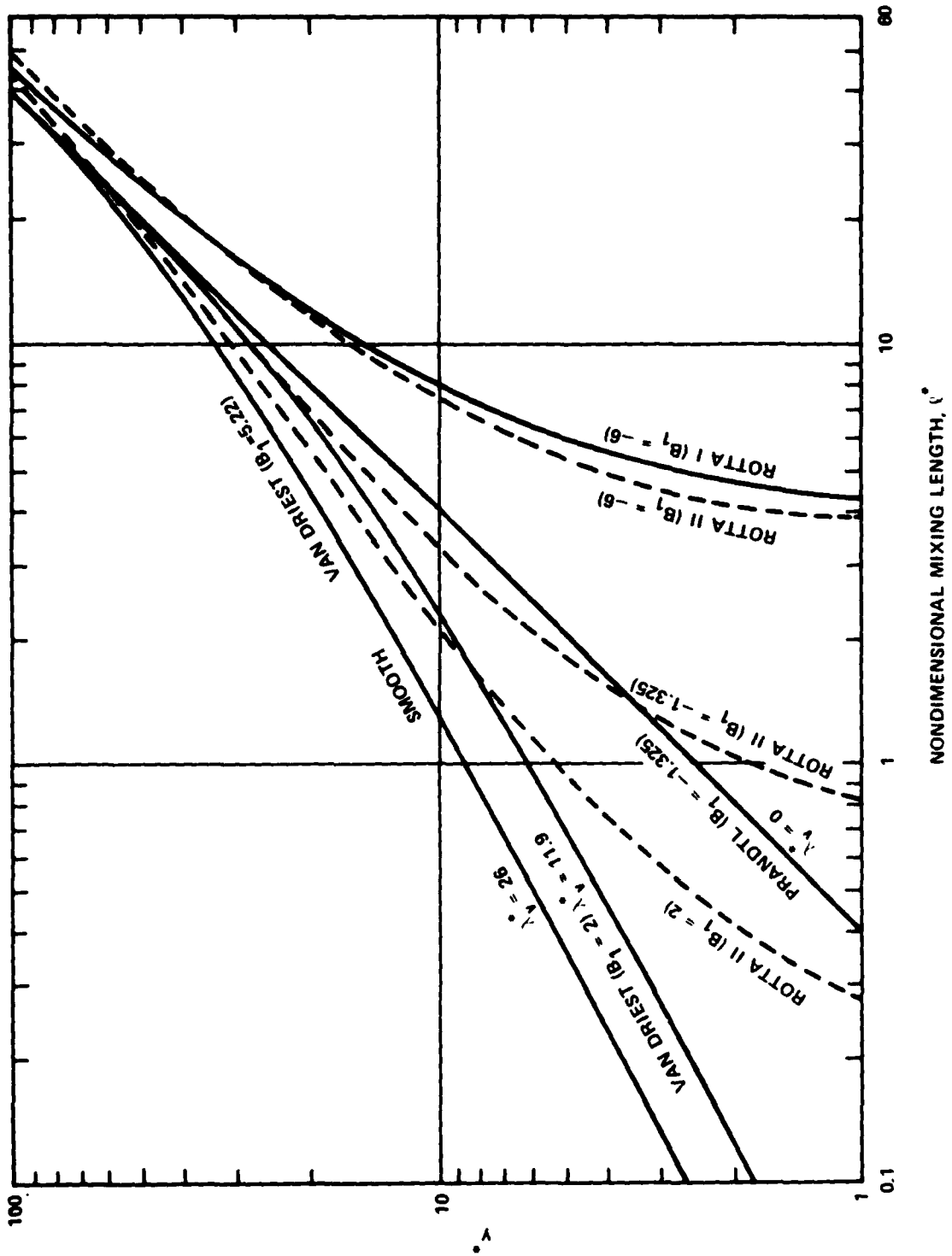


Figure 7 - Comparison of Mixing Lengths

APPENDIX A
CONVERSION OF MIXING LENGTHS TO EDDY VISCOSITIES

The concept of eddy viscosity ν_t (more properly eddy kinematic viscosity) was originally proposed during the last century by Boussinesq for turbulent flows as an analogy to the usual viscosity for laminar flows or

$$\frac{\tau_t}{\rho} = \nu_t \frac{du}{dy} \quad (\text{A.1})$$

Equating this to the turbulent shear stress given in terms of mixing lengths, Equation (7), produces the well known expression

$$\nu_t = \ell^2 \frac{du}{dy} \quad (\text{A.2})$$

Note that eddy viscosity unlike laminar viscosity is not a property of the fluid, but depends upon its position in the flow.

For various reasons it may be more desirable to relate eddy viscosity (ν_t) to mixing length without the presence of velocity gradient du/dy .

In general, shear stress (τ) has laminar and turbulent contributions such that

$$\frac{\tau}{\rho} = (\nu + \nu_t) \frac{du}{dy} \quad (\text{A.3})$$

Close to the wall $\tau \approx \tau_w$ and then, nondimensionally,

$$\frac{du^*}{dy^*} = \frac{1}{1 + \frac{\nu_t}{\nu}} \quad (\text{A.4})$$

Also from Equation (10)

$$\frac{du^*}{dy^*} = \frac{2}{1 + \sqrt{1 + (2\ell^*)^2}} \quad (\text{A.5})$$

Equating the two expressions for du^*/dy^* results in

$$\frac{v_t}{\nu} = \frac{1}{2} \sqrt{1+(2l^*)^2} - \frac{1}{2} \quad (\text{A.6})$$

This is the desired relation for converting mixing lengths to eddy viscosities.

At large values of l^* , $(v_t/\nu) \rightarrow l^* \rightarrow \kappa y^*$ or $v_t \rightarrow u_\tau l \rightarrow \kappa u_\tau y$.

For the van Driest formulation for arbitrarily rough surfaces, Figure A.1 shows the variation of eddy viscosity ratio v_t/ν with normal distance y^* . The smooth case is shown as well as the case for the boundary between the intermediate and fully rough regimes. Also, as an example of the fully rough regime v_t/ν is shown for $B_1 = -6$. At large values of y^* , $(v_t/\nu) \rightarrow \kappa y^*$ as seen in Figure A.1.

It is to be noted that the increase of v_t/ν with y^* presented here applies only to the boundary-layer region next to the wall. A limiting value is reached which corresponds to outer-region values such as those given by Cebeci and Smith.²

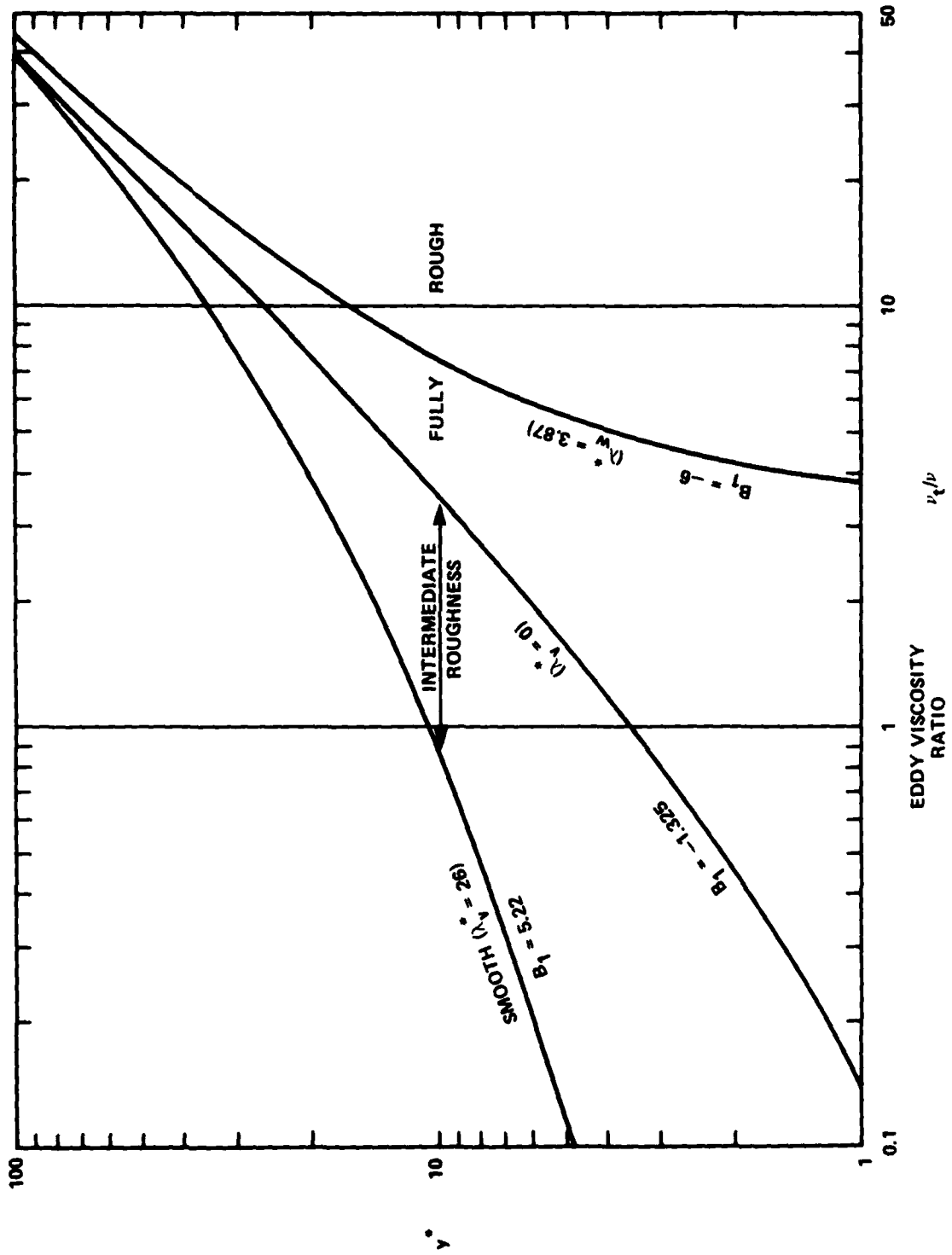


Figure A.1 - Eddy Viscosities Over Rough Surfaces

APPENDIX B
NEAR-WALL VALUES OF TURBULENT KINETIC ENERGY (k)
AND TURBULENT DISSIPATION RATE (ϵ)

A current modeling method for turbulence determines the turbulent shear stress from the eddy viscosity which, in turn, is obtained from the turbulent kinetic energy (k) and the turbulent dissipation rate (ϵ) from

$$v_t = c_\mu \frac{k^2}{\epsilon} \quad (\text{B.1})$$

where c_μ is a constant.

Values of k and ϵ are obtained from solutions of convection equations which are partial differential equations. However, close to the wall it has been found that values of k and ϵ obtained from mixing lengths may be used as inputs to the partial differential equations for k and ϵ with an improved accuracy⁶ in the solutions of the equations.

By equating the production and dissipation terms of the k -equation, Arora et al.⁶ related k and ϵ to the mixing length close to the wall as follows,

$$k = \frac{\ell^2}{\sqrt{c_\mu}} \left(\frac{du}{dy} \right)^2 \quad (\text{B.2})$$

and

$$\epsilon = \ell^2 \left(\frac{du}{dy} \right)^3 \quad (\text{B.3})$$

Elimination of the velocity gradient du/dy produces a direct relation between k and ϵ with ℓ as follows. First the relation for k and ϵ are nondimensionalized to

$$\frac{\sqrt{c_\mu}}{2} \frac{k}{u_\tau} = \ell^{*2} \left(\frac{du^*}{dy^*} \right)^2 \quad (\text{B.4})$$

and

$$\frac{\nu}{4} \frac{\epsilon}{u_{\tau}} = \ell^{*2} \left(\frac{du^*}{dy^*} \right)^3 \quad (\text{B.5})$$

Substitution of du^*/dy^* from Equation (10) produces

$$\frac{\sqrt{c_{\mu}}}{u_{\tau}^2} k = \left[\frac{2\ell^*}{1 + \sqrt{1 + (2\ell^*)^2}} \right]^2 \quad (\text{B.6})$$

and

$$\frac{\nu}{4} \frac{\epsilon}{u_{\tau}} = \ell^{*2} \left[\frac{2}{1 + \sqrt{1 + (2\ell^*)^2}} \right]^3 \quad (\text{B.7})$$

Some general properties of k and ϵ are now deduced. At higher values of ℓ^* , $(\sqrt{c_{\mu}}/u_{\tau}^2)k$ approaches 1 and $(\nu/u_{\tau}^4)\epsilon$ approaches $1/\ell^*$.

Also $(\nu/u_{\tau}^4)\epsilon$ reaches a maximum value of $1/4$ at $\ell^* = \sqrt{2}$.

This maximum value is independent of the mixing-length model.

In Figures B.1 and B.2, the variation of k and ϵ with y^* are shown for selected roughness conditions.

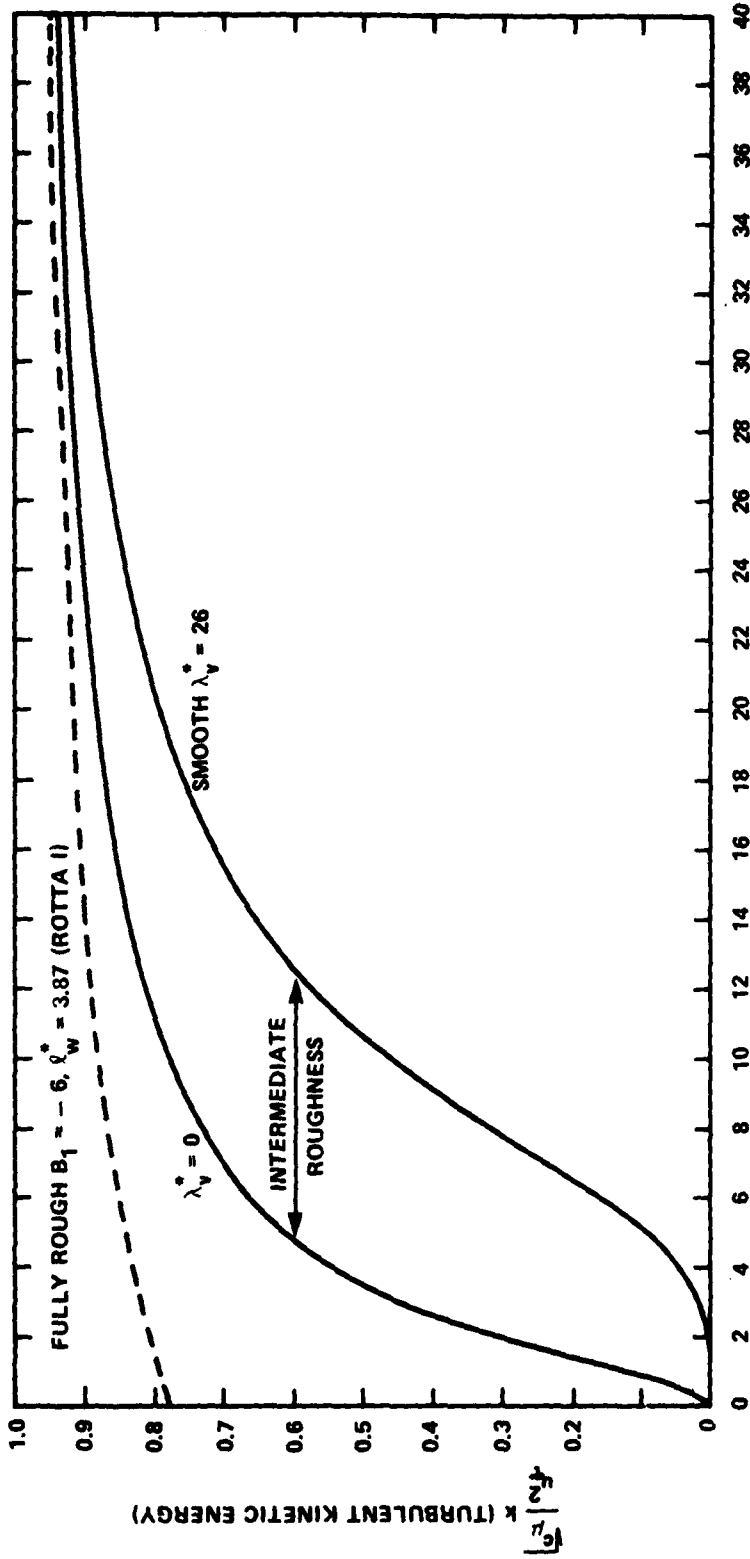


Figure B.1 - Variation of Turbulent Kinetic Energy Near Wall

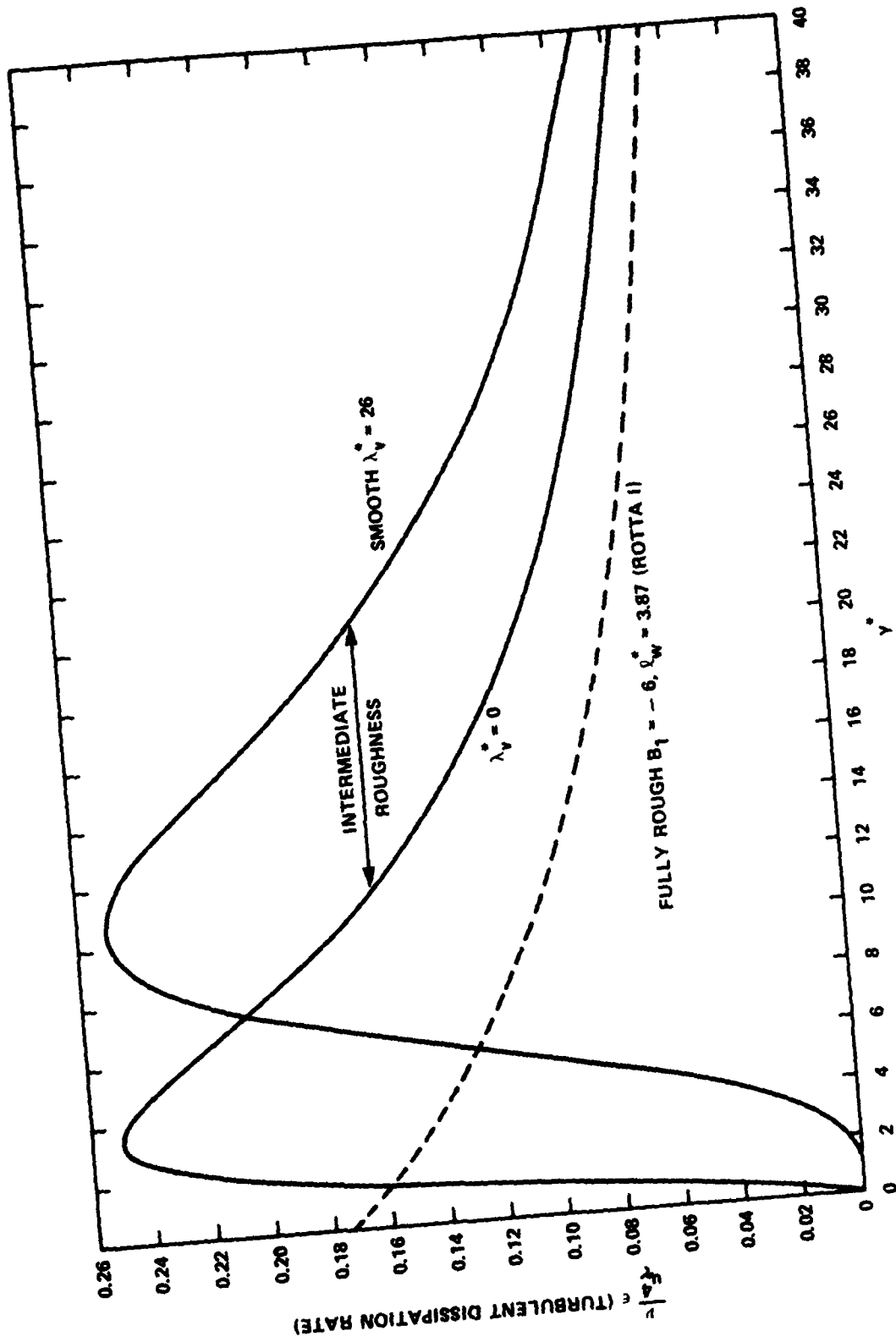


Figure B.2 - Variation of Turbulent Dissipation Rate Near Wall

APPENDIX C
HYPERBOLIC-TANGENT MODIFICATION FUNCTION

A hyperbolic-tangent function¹⁵ may be used as a modification function for arbitrarily rough surfaces.

$$M = \tanh (y^* / \lambda_h^*)^2 \quad (C.1)$$

The factor λ_h^* may be correlated with the roughness function B_1 in accordance with Equation (30). For $\lambda_h^* = 0$, $M = 1$ and $l^* = \kappa y^*$ which marks the limit of the intermediate roughness regime just as for the van Driest modifications function.

A comparison of the integrand $y^* (dI_2/dy^*)$ between the hyperbolic-tangent function and the van Driest function is shown in Figure C.1.

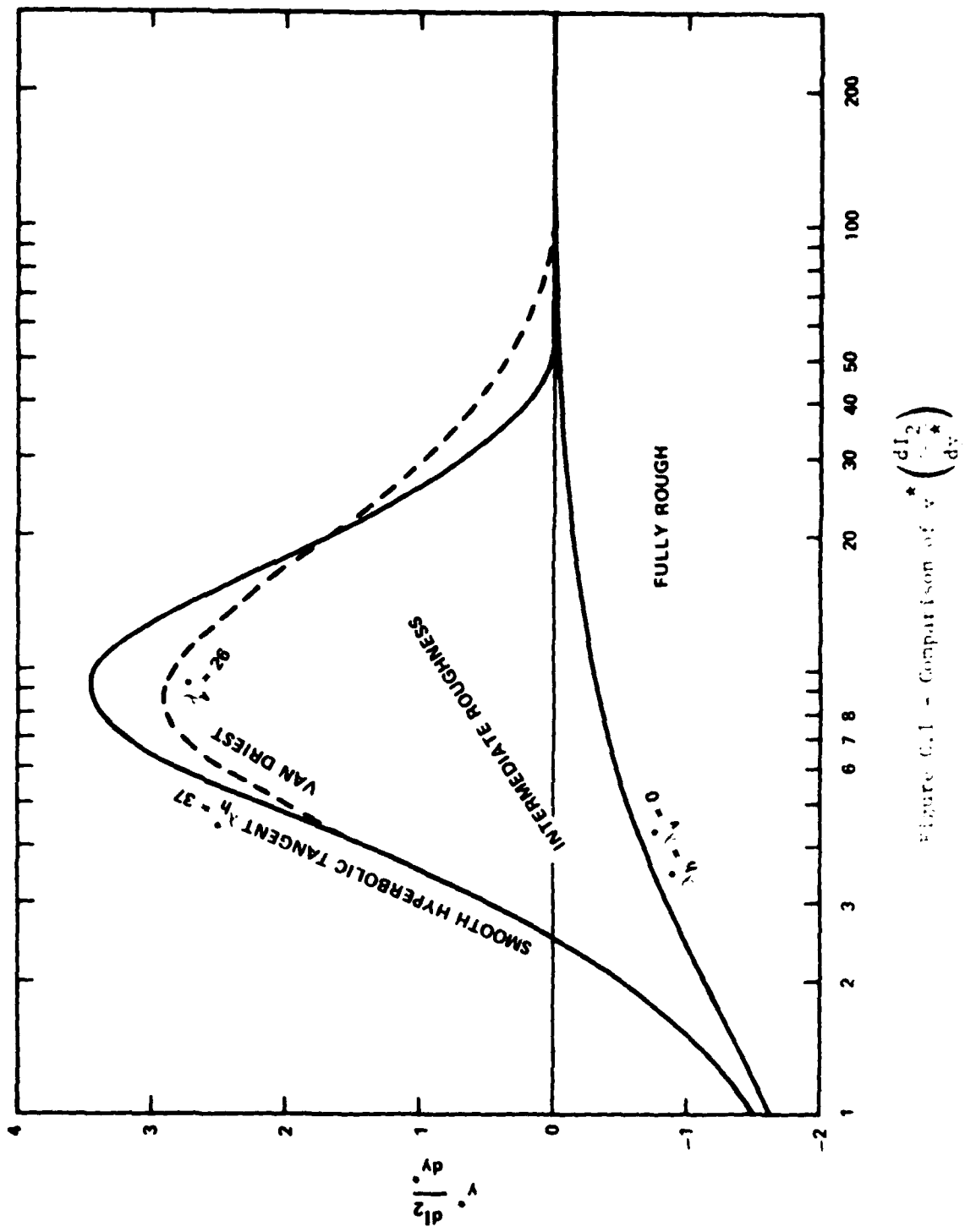


Figure 6.1 - Comparison of $v \cdot \left(\frac{dl_2}{dy} \right)$

REFERENCES

1. Patankar, S.V. and D.B. Spalding, "Heat and Mass Transfer in Boundary Layers," C.R.C. Press, Cleveland, Ohio (1968).
2. Cebeci, T. and A.M.O. Smith, "Analysis of Turbulent Boundary Layers," Academic Press, N.Y. (1974).
3. Nituch, M.J., S.S. Sjolander and M.R. Head, "An Improved Version of Cebeci-Smith Eddy-Viscosity Model," Aeronautical Quarterly, Vol. 29, Part 3, pp. 207-225 (Aug 1978).
4. Huang, T.T., N. Santelli and G. Belt, "Stern Boundary-Layer on Axisymmetric Bodies," 12th Symposium on Naval Hydrodynamics, National Academy of Sciences, Washington, D.C. (1979).
5. Sideman, S. and W.V. Pinczewski, "Turbulent Heat and Mass Transfer at Interfaces: Transport Models and Mechanisms," in "Topics in Transport Phenomena," C. Gutfinger, ed., pp. 47-207, Hemisphere Publishing Corporation, Washington, D.C. (1975).
6. Arora, R., K.K. Kuo and M.K. Razdan, "Near-Wall Treatment for Turbulent Boundary-Layer Computations," AIAA Journal, Vol. 20, No. 11, pp. 1481-1482 (Nov 1982).
7. Rotta, J., "Das in Wandnahe gültige Geschwindigkeitsgesetz turbulenter Stromungen," Ingenieur-Archiv, Vol. 18, pp. 277-280 (1950).
8. Rotta, J., "Turbulent Boundary Layers in Incompressible Flow," in "Progress in Aeronautical Sciences," Vol. 2, A. Ferri, D. Kuchemann and L.H.G. Sterne, eds., pp. 1-219, Pergamon Press, N.Y. (1962).
9. Cebeci, T. and K.C. Chang, "Calculation of Incompressible Rough-Wall Boundary-Layer Flows," AIAA Journal, Vol. 16, No. 7, pp. 730-735 (Jul 1978).
10. Nikuradse, J., "Laws of Flow in Rough Pipes," NACA TM 1292 (Nov 1950) (Translation from VDI-Forschungsheft 361, Jul/Aug 1933).
11. Hama, F.R., "Boundary-Layer Characteristics for Smooth and Rough Surfaces," Transactions, Society of Naval Architects and Marine Engineers, Vol. 62, pp. 333-358 (1954).

12. Granville, P.S., "The Frictional Resistance and Turbulent Boundary Layer of Rough Surfaces," *Journal of Ship Research*, Vol. 2, No. 3, pp. 52-74 (Dec 1958).
13. Granville, P.S., "Drag-Characterization Method for Arbitrarily Rough Surfaces by Means of Rotating Disks," *Journal of Fluids Engineering*, Vol. 104, No. 3, pp. 373-374 (Sep 1982).
14. van Driest, E.R., "On Turbulent Flow Near A Wall," *Journal of Aeronautical Sciences*, Vol. 23, pp. 1007-1011, 1036 (1956).
15. Patel, V.C., "A Unified View of the Law of the Wall Using Mixing-Length Theory," *Aeronautical Quarterly*, Vol. 24, Part 1, pp. 55-70 (Feb 1973).
16. Dahn, T., Personal Communication to T.C. Lin and R.J. Bywater, "Turbulence Models for High-Speed Rough-Wall Boundary Layers," *AIAA Journal*, Vol. 20, No. 3, pp. 325-333 (Mar 1982).

INITIAL DISTRIBUTION

Copies		Copies	
1	WES	15	NAVSEA (Continued)
1	U.S. ARMY TRAS R&D Marine Trans Div	1	55N2/A. Paladino
4	CHONR/432	4	55W3/W Sandberg, C. Chen, W. Livingstone, W. Patterson
	1 C.M. Lee	1	55W31/G. Jones
	1 R. Whitehead	1	55W/R. Keane, Jr.
	1 M. Reischman	1	55WX/F.S. Cauldwell
	1 A. Wood	1	56X1/F. Welling
3	NRL	1	56XP/F. Peterson
	1 Lib	1	63R31/T. Peirce
	2 Code 5844/R. Hansen, H. Wang	1	63Y312/R. Grady
		1	99612/Library
1	NORDA	12	DTIC
6	USNA	2	AFOSR
	1 Tech Lib	1	NAM
	1 Nav Sys Eng Dept	1	J.D. Wilson
	1 B. Johnson	1	AFFOL/FYS, J. Olsen
	1 T. Langan	2	MARAD
	1 M. McCormick	1	Div of Ship R&D
	1 Mech Eng Dept/J. Gillerlain	1	Lib
4	NAVPGSCOL	1	NASA, HQ/Lib
	1 Lib	2	NASA, Ames Res Ctr
	1 T. Sarpkaya	1	Lib
	1 J. Miller	1	M. Rubesin
	1 T. Houlihan	2	NASA, Langley Res Ctr
1	NADC	1	Lib
2	NOSC/Lib, D. Nelson	1	D. Bushnell (163)
3	NSWC, White Oak	5	NBS
	1 Lib	1	Lib
	2 Aero Res Br/W. Yanta, D. Auscherman	1	P.S. Klebanoff
1	NSWC, Dahlgren/Lib	1	G. Kulin
		1	H. Oser
2	NUSC/Lib, R. Nadolink	1	T.V. Vorburger
15	NAVSEA	1	NSF/Eng Lib
	1 05R24 (J. Sejd)	1	DOT/Lib TAD-491.1
	1 50151/C. Kennell		

Copies

2 MMA
 1 National Maritime Research
 Center
 1 Lib

1 Library of Congress/Science &
 Technology Div

4 U of Cal/Dept Naval Arch,
 Berkley
 1 Lib
 1 W. Webster
 1 J. Paulling
 1 J. Wehausen

1 Case Western Reserve U/
 E. Reshotko, Mech Eng

5 CIT
 1 Aero Lib
 1 T.Y. Wu
 1 A.J. Acosta
 1 R.H. Sabersky
 1 D. Coles

3 Colorado State U.
 1 Eng Res Ctr
 2 Civil Eng Dept/V. Sandborn,
 W.Z. Sadeh

1 U of Conn/V.E. Scottron

2 Cornell U
 1 Shen
 1 J.L. Lumley, Mech Eng

2 Harvard U
 1 G. Carrier
 1 Gordon McKay Lib

1 U of Ill at Chicago/J.P. Hartnett

7 U of Iowa/Inst of Hydraulics
 1 Lib
 1 L. Landweber
 1 J. Kennedy
 1 V.C. Patel
 1 B.R. Ramaprian
 1 F. Stern
 1 O. Sarda

Copies

1 Lehigh U/D.E. Abbott, Mech Eng

2 U of Maryland
 1 A. Gessow, Aero
 1 A. Plotkin, Aero

5 MIT
 1 Lib
 1 J.R. Kerwin
 1 P. Leehey
 1 J.N. Newman
 1 M.T. Landahl

4 U of Minn/St. Anthony Falls
 1 Lib
 1 R. Arndt
 1 J. Wetzel
 1 E. Silberman

5 U of Mich/NAME
 1 Lib
 1 W. Vorus
 1 R. Couch
 1 S. Cohen
 1 W.W. Willmarth (Aerosp)

1 U of Mississippi/J.A. Fox,
 Mech Eng

1 Mississippi St U/B.K. Hodge,
 Mech Eng

1 Ohio St U/J.L. Eakin, Chem Eng

4 Penn State/ARL
 1 B.R. Parkin
 1 R.E. Henderson
 1 ARL Lib
 1 B. Lakshminarayana (Aerosp)

2 Princeton U/Mellor, Hama

2 U of Rhode Island
 1 F.M. White
 1 T. Kowalski (Ocean Eng)

Copies

2 Science Application, Inc.
Annapolis, MD
1 C. von Kerczek
1 G.H. Christoph

3 SIT
1 Lib
1 J. Breslin
1 D. Savitsky

7 Stanford U
1 J. Johnston, Dept Mech Eng
1 S.J. Kline, Dept Mech Eng
1 W. Reynolds, Dept Mech Eng
1 Eng Lib
1 R. Street, Dept Civil Eng
1 E.Y. Hsu, Dept Civil Eng
1 T.K. Cheung, Dept Civil Eng

1 Texas A&M U/R.H. Page, Mech Eng

1 U of VA/Aero Eng Dept

1 Union College/J.R. Shanebrook,
Mech Eng

3 VPI
1 J. Schetz, Dept Aero &
Ocean Eng
1 H. Moses, Mech Eng
1 D. Telionis, Eng Sci

1 Washington St U/J.A. Roberson,
Eng

5 Webb Inst
1 Lib
1 Lewis
1 Ward
1 N. Hamlin
1 J. Hadler

2 U of Hawaii/Ocean Eng
1 M. St. Denis
1 J. Craven

Copies

2 U of Houston
1 C. Dalton (Mech Eng)
1 A. Kareem (Civil Eng)

4 Purdue U/Mech Eng
1 V. Goldschmidt
1 A. McDonald
1 W. Tiederman
1 K.T. Paw U (Agronomy)

1 San Diego St U (Mech Eng)
1 J. Hoyt

1 Southern Methodist U/
R.L. Simpson, Mech Eng

1 U of Cal/Santa Barbara
1 M.P. Tulin (Mech Eng)

1 U of Bridgeport
1 E. Uram (Mech Eng)

1 U of Delaware
1 J. Wu (Marine Studies)

1 SNAME/Tech Lib

1 A.R.A.P. (McLean, VA)/
C. Donaldson

1 Analytical Methods (Bellevue,
WA)/F.A. Dvorak

1 Bell Aerospace

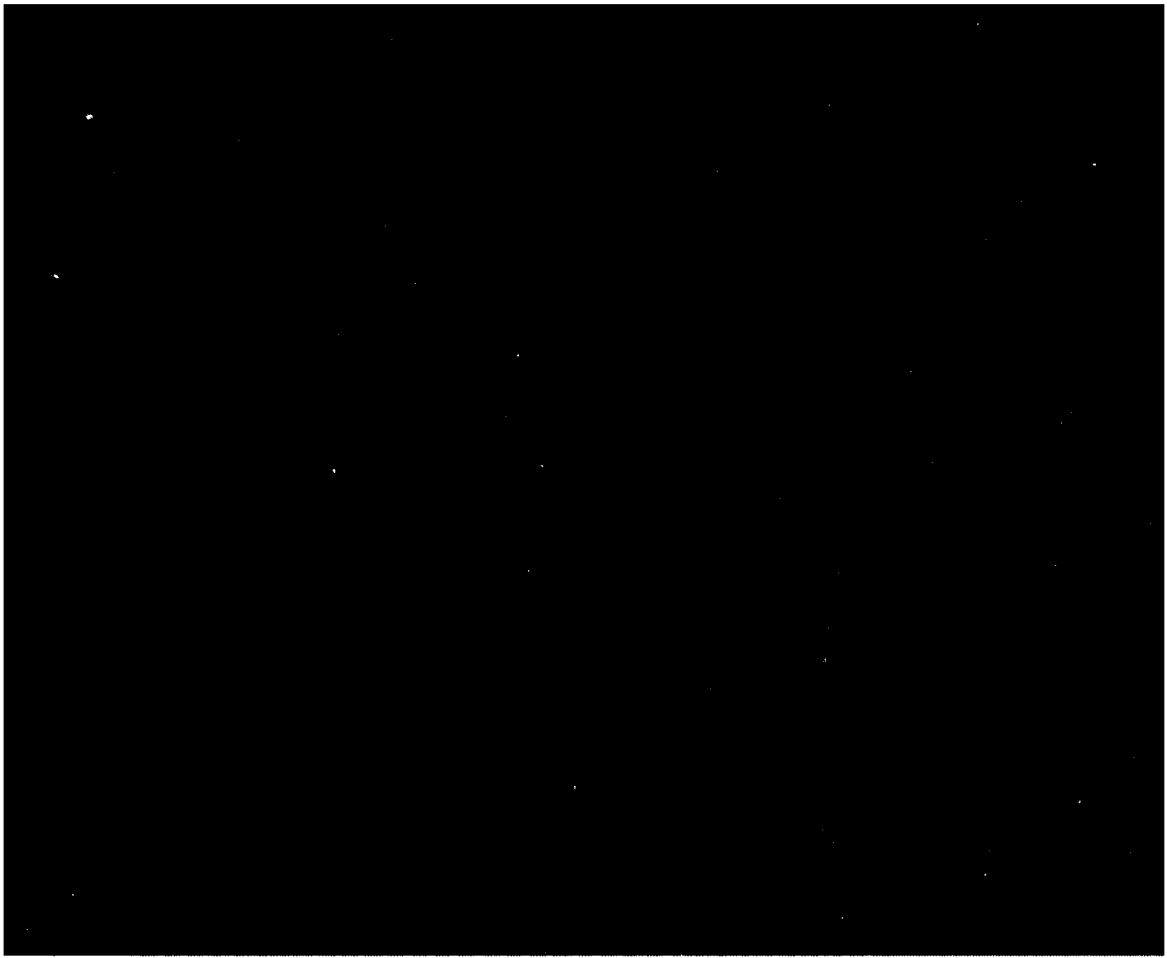
2 Boeing Company/Seattle
1 Marine System
1 P. Rubbert

1 Bolt, Beranek & Newman/Lib

1 Dynamics Tech (Torrance, CA)/
G.L. Donohue

1 Exxon, NY/Design Div
Tank Dept

Copies		Copies	
1	Exxon Math & System, Inc.	2	Vought Advanced Tech Cen (Dallas, TX)
1	General Dynamics, FB/Boatwright	1	G.R. Hough
1	Flow Research	1	C.S. Wells Jr.
1	Gibbs & Cox/Tech Info		CENTER DISTRIBUTION
2	Grumman Aerospace Corp	Copies	Code Name
	1 Lib	1	0120 D. Moran
	1 R.E. Melnik		
4	Hydronautics	1	15 W.B. Morgan
	1 Lib	1	152 W.C. Lin
	1 E. Miller	1	1521 W. Day
	1 V. Johnson	1	1521 E. West
	1 R. Barr	1	1522 G. Dobay
1	Lockheed, Georgia/J.F. Nash	1	1522 M. Wilson
1	Lockheed, Sunnyvale/Waid	1	1522 D. Jenkins
2	McDonnell Douglas,	1	154 J. McCarthy
	Long Beach, CA	25	1540 P. Granville
	1 T. Cebeci	1	1544 R. Boswell
	1 J. Hess	1	156 D. Cieslowski
1	McDonnell Douglas (St. Louis, MO)/R.J. Hakkinen	1	156 G. Cox
1	Northrop Corp/Aircraft Div	1	1564 J. Feldman
1	NKF Engineering Assoc. (Arlington, VA)/J. Malone	1	1606 T.C. Tai
2	Rand Corp/J. Aroesty, W. King	1	1802 H.J. Lugt
1	Sun Shipbuilding/Chief Naval Arch	1	184 J. Schot
1	Scientific Res Assoc (Glastonbury, CT)/H. McDonald	1	1843 H. Hausssling
1	United Technology/East Hartford, CT	1	19 M.M. Sevik
1	Westinghouse Electric	1	194 J.T. Shen
		1	1940 M.J. Casarella
		10	5211.1 Reports Distribution
		1	522.1 TIC (C) (1 m)
		1	522.2 TIC (A)



LMED
— 8